VIP Heterogeneous Catalysis

DOI: 10.1002/anie.201102617

Highly Efficient and Stable $CeNiH_ZO_Y$ Nano-Oxyhydride Catalyst for H_2 Production from Ethanol at Room Temperature**

*Cyril Pirez, Mickaël Capron, Hervé Jobic, Franck Dumeignil, and Louise Jalowiecki-Duhamel**

Dedicated to the Fritz Haber Institute, Berlin, on the occasion of its 100th anniversary

Hydrogen and fuel cells are crucial to any clean energy policy. At the international level, hydrogen has been proposed as a major energy vector that could contribute to the reduction of the global dependence toward fossil fuels and to the lowering of greenhouse-gas emissions and atmospheric pollution.[1] At present steam reforming of hydrocarbon compounds, that is, natural gas, is the most commonly used and generally the most economically competitive method for hydrogen production. Producing hydrogen in a sustainable way from an environmentally friendly and promising renewable source of hydrogen is highly desired for the growing fuel-cell technology and industrial needs. Bioethanol obtained from biomass has been proposed as a promising renewable source of hydrogen for these systems by simultaneously addressing the greenhouse-effect issue.[2] In such a context, it is today a major challenge to provide low-cost catalysts that are able to efficiently break the C–C bond from bioethanol. Materials, such as catalysts or electrocatalysts that are able to activate fuels like H_2, and alcohols are absolutely required for the development of new technologies.[3]

The endothermic steam reforming of ethanol (SRE) given by Reaction (1) requires energy input,[4] which leads to high operation costs and to a nonadvantageous global CO_2 balance. However, the required energy can be supplied by adding some oxygen or air in the feed. This enables the exothermic partial oxidation of ethanol (POE) given by Reaction (2),[5] during which a portion of ethanol is burnt, providing the energy needed to simultaneously realize the SRE in Reaction (1).[6] Such a technology would be suitable for onboard hydrogen production, that is, for mobile applications, which require high hydrogen selectivity and rapid response.

$$C_2H_5OH + 3H_2O \rightarrow 6H_2 + 2CO_2 \quad (1)$$

$$C_2H_5OH + 1.5O_2 \rightarrow 3H_2 + 2CO_2 \quad (2)$$

Here, we show that H_2 is produced from ethanol in a sustainable way by taking advantage of the chemical energy delivered from the reaction between hydride species of the nano-oxyhydride catalyst and O_2. We have successfully developed a new technology that saves energy because of the exothermic reaction between hydride species of the catalyst and O_2 (chemical energy) and the exothermic reaction between ethanol and O_2 (partial oxidation). The chemical reactions provide the energy necessary to convert ethanol and produce H_2. To this purpose we developed a highly active, selective, stable, and cost-effective catalyst. We report that the low-cost $CeNiH_ZO_Y$ nano-oxyhydride catalyst efficiently split the C–C bond of ethanol at room temperature, which is a major advance in the field. The $CeNiH_ZO_Y$ nano-oxyhydride catalyst has the remarkable ability of simultaneously activating ethanol, producing H_2, and providing hydride species to sustain the chemical reaction with O_2.

The active $CeNiH_ZO_Y$ nano-oxyhydride catalyst is obtained by in situ pretreatment of a $CeNiO_Y$ nanocompound with H_2 at 250 °C for 10 h. The $CeNiH_ZO_Y$ catalyst (0.03 g of the starting material) has been tested for hydrogen production from ethanol in simultaneous presence of water and O_2 (the ratio of $EtOH/H_2O/O_2/N_2$ was 1:3:1.6:1.3). Figure 1

[*] Dr. C. Pirez, Dr. M. Capron, Prof. F. Dumeignil, Dr. L. Jalowiecki-Duhamel
Université Lille Nord de France, 59000 Lille (France)
and
CNRS UMR8181, Unité de Catalyse et Chimie du Solide, UCCS
59655 Villeneuve d'Ascq (France)
E-mail: louise.duhamel@univ-lille1.fr
Homepage: http://uccs.univ-lille1.fr
Prof. F. Dumeignil
Institut Universitaire de France, Maison des Universités
10, Boulevard Saint-Michel, 75005 Paris (France)
Dr. H. Jobic
IRCELyon Institut de Recherche sur la Catalyse
et l'Environnement de Lyon
2 avenue Albert Einstein, 69626 Villeurbanne Cedex (France)

[**] This work was financially supported by the CNRS, the French Ministry (C. Pirez grant), and the Institut Laue Langevin (ILL) Grenoble, France.

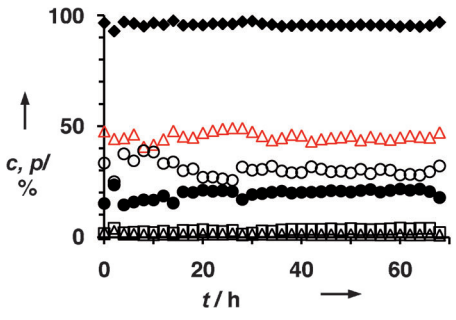

Figure 1. Ethanol conversion (*c*, ◆) and distribution of gas-phase products (*p*: production, H_2 △, CO_2 ○, CO ●, CH_4 △, and CH_3CHO □ in mol%) obtained versus time over the $CeNiH_ZO_Y$ oxyhydride catalyst (0.03 g) with an oven temperature at 60 °C. The composition of the reaction mixture $EtOH/H_2O/O_2/N_2$ is 1:3:1.6:1.3 and the measured reaction temperature is of 280 °C.

shows the ethanol conversion rate and the molar fraction of H_2 calculated relatively to the gas-phase products. The results reported at a reaction temperature of 280 °C are obtained with a much lower oven temperature of 60 °C. The ethanol conversion is almost complete at a H_2 production of about 45 % relative to all gas-phase products. The other products are mainly CO_2 and CO (Figure 1). To our knowledge, the obtained results are the best results reported up-to-date for a low-cost catalyst.[4a] It must be noted that the catalytic reaction must be initiated at 230 °C. After an induction period of a few minutes (around 5 min.), the temperature increases and then only a small energy supply is needed to maintain the reaction, and therefore the oven temperature is lowered to 60 °C. The exothermic reaction between hydride species of the catalyst and O_2 (chemical energy) and the exothermic reaction of ethanol and O_2 is used to provide the energy necessary to convert ethanol and produce H_2. The activity is remarkably stable after 70 h of reaction even if some solid carbon is formed (63 mg per gram of catalyst and hour). The stability is certainly due to the filamentous type of carbon formed.

Compared to previous results reported by us under conditions of SRE, the conversion is largely increased when adding O_2 to the reaction mixture. Even if a high and stable activity (5 h) was already observed under conditions of SRE at a conversion rates of 50 % of ethanol and about 50 % of H_2 formed at 250 °C over 0.2 g of the catalyst.[7] The high activity of the cerium–nickel-based catalysts has already been reported and attributed to the existence of strong interactions between Ni and Ce species.[4a,7] In the laboratory, $CeNi_XO_Y$ mixed oxides were largely studied because of the strong interactions existing between Ni and Ce species in the solid. Redox processes between Ce^{4+}, Ce^{3+}, Ni^0, and Ni^{2+} were shown. The active Ni species are characteristically and easily reduced and reoxidized because of their close interaction with Ce species, for which particular active sites have been proposed.[8]

The ethanol conversion and hydrogen production have been studied versus the O_2/EtOH ratio, that is, the O_2 concentration, because the ethanol concentration was kept constant. An increase in temperature when the O_2 concentration was increased has also been measured (Figure 2). Therefore, the oven temperature was fixed at 200 °C and the

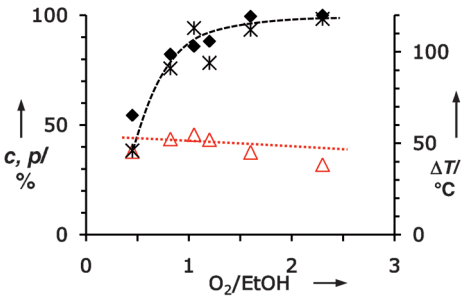

Figure 2. Ethanol conversion (c; ◆) and H_2 production (p; △) over $CeNiH_ZO_Y$ (0.2 g) in a mixture of EtOH/H_2O/O_2. The ratio of H_2O/EtOH is kept at 3:1. The oven temperature is fixed at 200 °C and the variation of temperature (ΔT) is measured (*).

H_2O/EtOH ratio was kept at 3:1. Each point reported in Figure 2 is obtained after 5 h of reaction over a fresh solid (0.2 g) pre-treated in H_2 at 250 °C. For an O_2/EtOH ratio larger than 1:1, the variation of temperature (ΔT) is almost constant (increase of about 120 °C) at total conversion of ethanol. It seems that there is a limitation because of the total conversion of ethanol. As presented in Figure 1 with a much lower catalytic mass (0.03 g) and a ratio of 1.6:1 the variation of temperature is much higher. So the limitation is a result of the low proportion of ethanol relative to the catalytic mass. Without pre-treatment of the catalyst with H_2 under exactly the same conditions, we did not observe a variation of temperature. Therefore, even if the contribution of the exothermic partial oxidation reaction must also be considered, this contribution cannot explain the results obtained. Moreover, to our knowledge such a phenomenon has not been reported in the literature.

Addition of O_2 leads to an increase in the conversion of ethanol while the percentage of formed H_2 remains almost constant up to an O_2/EtOH ratio of 1.2:1 (Figure 2). For higher O_2/EtOH ratios, the formation of H_2 slightly decreases. The relative quantities of acetaldehyde, CO, and methane decrease when the O_2 concentration is increased (Figure 3).

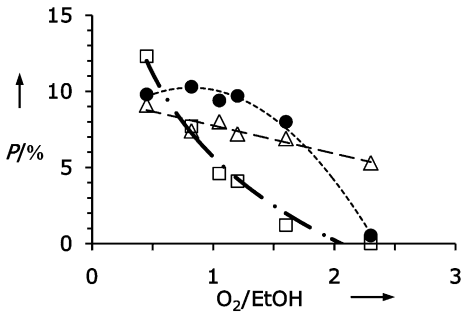

Figure 3. Product distribution (P) obtained over $CeNiH_ZO_Y$ in a EtOH/H_2O/O_2 reaction mixture with an oven temperature fixed at 200 °C. CH_3CHO (□), CH_4 (△), and CO (●) in the gas phase (mol %). The ratio of H_2O/EtOH is kept at 3:1.

This is also the case for acetone (not reported) formed in small quantities (2.5 %) only at an O_2/EtOH ratio of 0.5:1. As expected, the CO_2 quantity (not reported) increases from 30 to 60 % at the highest O_2 concentration. An O_2/EtOH ratio of about 1.2:1 leads to a high ethanol conversion with the highest yield of H_2 but some acetaldehyde is still obtained. At an O_2/EtOH ratio of 1.6:1 a high yield of H_2 is obtained without formation of acetaldehyde, which is a good compromise.

Dehydrogenation of ethanol produces acetaldehyde and H_2 [Reaction (3)], whereas decomposition of ethanol (and/or acetaldehyde) produces methane, carbon monoxide, and hydrogen [Reaction (4)].

$$C_2H_5OH \rightarrow C_2H_4O + H_2 \quad (3)$$

$$C_2H_5OH \rightarrow CH_4 + CO + H_2 \quad (4)$$

The diffraction patterns obtained from the calcined $CeNiO_Y$ catalyst (before pretreatment with H_2) suggests the

presence of two phases, a ceria-like phase (JCPDS file: 34-0394) and a crystallized NiO phase (JCPDS file: 4-0835; Table 1).

Table 1: Surface area and crystallites size.

Catalyst	Ni [wt%]	SA[a] [$m^2 g^{-1}$]	d (CeO_2)[b] [nm]	d (NiO)[b] [nm]
$CeNiO_Y$	20	94	5	10

[a] BET specific surface area. [b] Deduced from XRD.

In previous studies, we reported that some small NiO nanoparticles (around 2 nm)[8d] coexist with larger NiO nanoparticles (10 nm) observed by XRD (Table 1).[8a] Therefore, the $CeNiO_Y$ catalyst, which possesses a specific surface area of 94 $m^2 g^{-1}$, corresponds to a nanocompound of CeO_2 particles about 5 nm in diameter and NiO nanoparticles of different sizes. CeO_2 can be modified by the insertion of Ni species but it has been shown that for this specific Ni content ($CeNiO_Y$), the solid solution is obtained in low proportion.[8a] To activate Ni species belonging to small NiO nanoparticles (and/or in solid solution), the required temperature for pretreatment with H_2 corresponds to the first temperature-programmed reduction (TPR) peak (Figure 4).[7a] It has been shown that a higher temperature for pretreatment with H_2 leads to a decrease in the conversion of ethanol at low temperature under conditions of SRE.[7b]

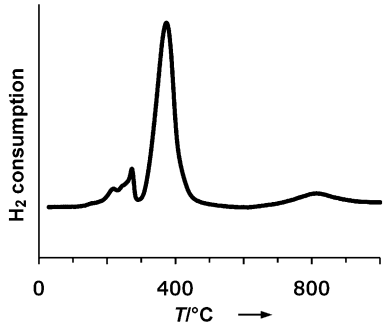

Figure 4. Temperature-programmed reduction of $CeNiO_Y$ in H_2.

The pretreatment with H_2 at 250 °C leads to the formation of an oxyhydride compound. As a matter of fact, chemical titration of the hydrogen species stored in the solid has shown previously that $CeNi_XO_Y$ mixed oxides store high quantities of hydrogen, and among the studied series, the $CeNi_1O_Y$ compound has been found to store the highest quantity of reactive hydrogen.[8b,c] To explain the process of hydrogen storage it has been proposed that hydrogen can be heterolytically dissociated at an anionic vacancy and a O^{2-} species of the catalyst [Reaction (5)]

$$O^{2-}M^{n+}\square + H_2 \rightarrow OH^- M^{n+}H^- \quad (5)$$

with $\square$: anionic vacancy and M^{n+}: cation. It has been reported that metallic nickel adsorbs hydrogen;[9] therefore, for the cerium–nickel system, in addition to the route described above, the homolytic dissociation of H_2 on Ni^0 has also been considered, and different hydrogen species can coexist.[8a] However, the in situ XRD analysis of H_2 does not evidence Ni^0 species at a temperature of 250 °C for 10 h and even at 260 °C for 10 h (Figure 5). On the studied compound, metallic Ni is observed by XRD for a treatment with H_2 at 300 °C.

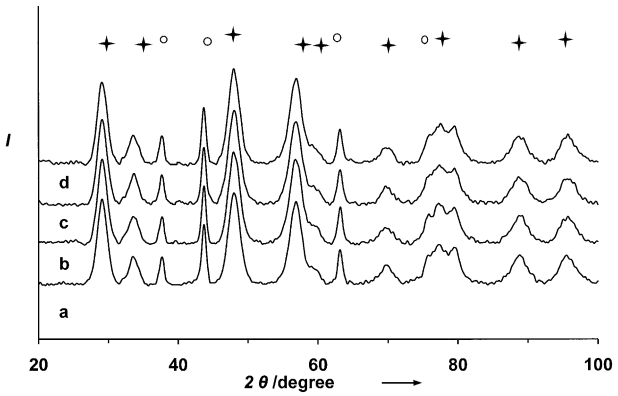

Figure 5. XRD patterns of $CeNiO_Y$ obtained during in situ reduction in H_2 at a) 250 °C, b) 250 °C for 10 h, c) 260 °C, and d) 260 °C for 10 h. Peaks assigned to CeO_2 (+) and NiO (○).

The insertion of hydride species into the solid is well shown by inelastic neutron scattering (INS).[10] The treatment with H_2 generates an increase in the level of the INS spectrum as well as the emergence of new peaks associated to vibration bands of hydrogen (Figure 6). The level of the spectrum is

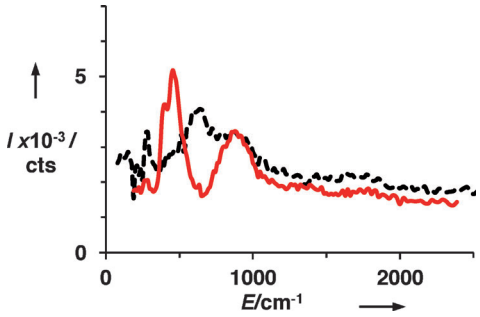

Figure 6. INS spectrum of $CeNiH_2O_Y$ (red solid line) treated in H_2 at 250 °C after subtraction of the the $CeNiO_Y$ spectrum, and INS spectrum of $CeNiH_2O_Y$ after oxidation and subtraction of the $CeNiO_Y$ spectrum (dashed line).

proportional to the hydrogen content. The INS spectrum of $CeNiO_Y$ (treated in vacuum at 200 °C) evidences some hydrogen species with vibration bands at about 250, 400, and 630 cm^{-1}, which are already present in the calcined compound.[11] As a matter of fact, this mixed oxide contains hydroxy groups before treatment with H_2.

Two new intense and large bands at about 460 and 870 cm^{-1} are observed on the catalyst treated with H_2 because of the insertion of different hydrogen species. To observe more precisely the hydrogen species created by treatment

with H_2 for activation, the INS spectrum of $CeNiO_Y$ in Figure 6 has been subtracted from that of $CeNiH_ZO_Y$ (treated in H_2 at 250 °C). The hydride species related to the peak at about 460 cm^{-1} appear clearly after treatment with H_2 at 250 °C. The large band at 870 cm^{-1} was assigned to hydrogen species interacting with metallic nickel Ni^0 species.[11] Even if Ni^0 species are not observed by XRD, some small particles can exist, which are not visible by XRD because of the limit of detection. However, the concentration of the hydrogen species related to the band at 870 cm^{-1} decreases when the Ni loading is decreased, and it disappears when the Ni/Ce ratio is 0.5:1 (Figure 7), which is in agreement with the existence of a high proportion of solid solution of cerium and nickel in this compound.[8a]

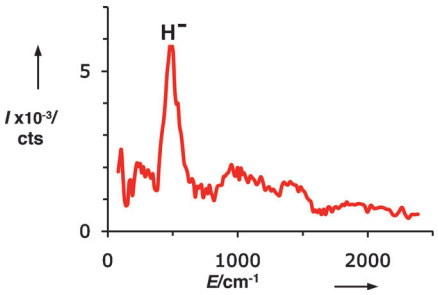

Figure 7. INS spectrum of $CeNi_{0.5}H_ZO_Y$ treated in H_2 at 250 °C after subtraction of the $CeNi_{0.5}O_Y$ spectrum.

The same phenomenon (exothermicity) is observed in the absence of hydrogen species corresponding to the band at 870 cm^{-1}. When the oxyhydride is re-oxidized at ambient temperature in air, the reaction is exothermic and the peak related to hydride species disappears, whereas an intense large band at 630 cm^{-1} appears, which is assigned to the formation of hydroxy groups (Figure 6). This finding is in good agreement with the existence of highly reactive hydride species leading in the presence of O_2 to the formation of hydroxy groups [Reaction (6)]. When the solid is pumped several times, these hydroxy groups can be eliminated (water) and the spectrum obtained is the same as the one observed for the calcined $CeNiO_Y$ solid.

$$H^- + 1/2\,O_2 \rightarrow OH^- \qquad (6)$$

The ethanol dehydrogenation step requires the abstraction of hydrogen species from an alcohol, which is the rate-determining step. Therefore, the ability of the solid to accept hydrogen is an important factor. The measured variation of temperature can be mainly attributed to the reaction between hydride species of the solid with O_2 (exothermic) and the variation of temperature depends on the concentration of hydrogen stored in the solid in the form of hydrides. This phenomenon allows the decrease of the oven temperature. A part of hydride species formed from ethanol react with O_2, providing chemical energy, which maintains the catalytic reaction. The reaction is sustainable because hydride species are replaced and provided by ethanol. Finally, as it has been proposed for heterolytic dissociation of H_2 [Reaction (5)], an active site involving an anionic vacancy and an O^{2-} species of the solid can be envisaged for the heterolytic dissociation of ethanol [Reaction (7)].

$$O^{2-}M^{n+}\square + C_2H_5OH \rightarrow OH^-M^{n+}H^- + C_2H_4O \qquad (7)$$

Such a site has already been modeled, as shown in Scheme 1, by an ensemble of two cations in close interaction. Three coordinatively unsaturated sites (3 CUS, ^3M) are a

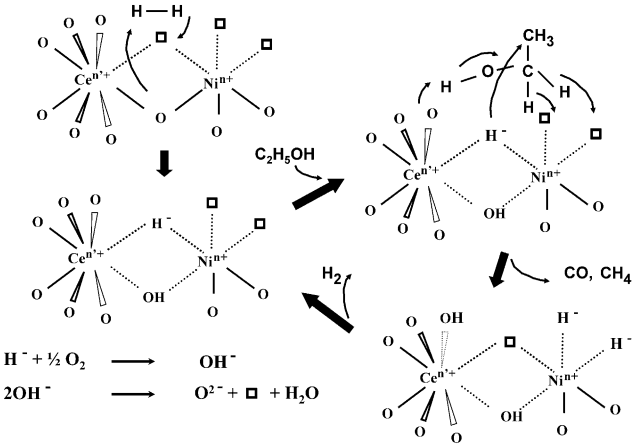

Scheme 1. Mechanism and active-site modeling for ethanol transformation over $CeNiH_ZO_Y$ nano-oxyhydride. (Ni^{n+}: Ni^{2+} or $Ni^{\delta+}$ and $Ce^{n'+}$: Ce^{4+} or Ce^{3+})

prerequisite for alkadiene hydrogenation activity, and different ensembles $^XM{-}^YM'$ (where X and Y are the numbers of unsaturations (anionic vacancies) on each cation) have been proposed to be the active sites, each elementary ensemble being associated with a particular reaction.[8b,c] Depending on the unsaturation degree of this active site, conversion of ethanol can lead to different products. In Scheme 1 the ^{3}Ni–^{1}Ce site leads to the formation of H_2, CO, and CH_4. At a lower number of anionic vacancies on the site, acetaldehyde and H_2 can be obtained by heterolytic abstraction of hydrogen. At a higher number of anionic vacancies on the site (^{3}Ni–^{3}Ce) obtained after treatment with H_2 at 250 °C, ethanol can be converted to H_2, CO, and carbon. As a matter of fact, H_2 production from CH_4 has been proposed for this kind of catalyst.[8d] This finding is in agreement with the observed increase of O vacancies induced by doping ceria with Ni[4a,8a,12] even if the existence of a hydride species has not been envisaged.[4a]

In conclusion, we have successfully developed a new route for hydrogen production that saves energy by smartly combining chemical reactions which take advantage of the reactivity of hydride species stored in active $CeNiH_ZO_Y$ nano-oxyhydride catalysts. We believe that our discoveries may be general and can be applied to many other processes. Our findings will motivate further fundamental theoretical and experimental studies and will lead to new exciting developments.

Experimental Section

The $CeNiO_Y$ nanocompound was prepared by coprecipitation of the corresponding hydroxides from mixtures of cerium and nickel nitrates (0.5 M) using triethylamine as a precipitating agent. After filtration, the solid was dried at 100 °C and calcined in air at 500 °C for 4 h. The loading was measured by microanalysis and the specific surface area (SA) by the Brunauer–Emmett–Teller (BET) method (Table 1).

XRD analysis was carried out with a D 5000 Siemens diffractometer. The crystallites size was calculated, using the Halder–Vagner–Langford equation, from the most intense reflections observed for the NiO and CeO_2 crystallographic structures.

TPR was performed on a Micromeritics Autochem 2920 analyzer, and the hydrogen consumption was measured using a thermal conductivity detector (TCD): 0.05 g of the sample were treated in a H_2 (5 %)/Ar (95 %) gas mixture (2 $L\,h^{-1}$). The temperature was increased to 800 °C at a heating rate of 10 °C min^{-1}.

Inelastic neutron scattering (INS) experiments were performed using the IN1 BeF spectrometer at the Institut Laue Langevin, Grenoble. The solid (36 g) was placed in a stainless steel container and the treatment with H_2 (10 h) was performed using gas of high purity. INS experiments were carried out at 10 K using a Cu (200) monochromator for energy transfers between 80 and 380 cm^{-1} and a Cu (220) monochromator for energy transfers between 380 and 3000 cm^{-1}. The scattering cross-section is much greater for hydrogen (80 barns) than for other elements (5 barns), therefore, INS emphasizes motions of hydrogen species.

The catalytic performances were measured at atmospheric pressure with a quartz fixed-bed reactor (inner diameter 4 mm) fitted in a programmable oven, in the temperature range of 60–500 °C. The catalyst was previously treated in situ with H_2 at 250 °C for 10 h to form the oxyhydride. The water/ethanol mixture (molar ratio 3:1) was pumped and vaporized in a preheating chamber. The O_2/ethanol molar ratio was varied between 0.5:1 up to 2.5:1. The ethanol/water/O_2/N_2 gas stream (total flow: 60 mL min^{-1}) was then fed to the reactor. The catalyst (0.2 g) was diluted in SiC and sandwiched between four layers of SiC. Almost the same effect has been obtained without dilution. The gases at the outlet of the reactor were analyzed on-line by gas chromatography using flame ionization (FID) and thermal conductivity detectors. The reaction data were collected as a function of time and reported after 5 h at each temperature. Solid carbon was formed as reported.

The reactants must be introduced in a specific order and O_2 must be introduced at last to avoid re-oxidation of the oxyhydride. When the reactants were introduced in the reactor, the reactor temperature significantly varied, depending on the ability of the oxyhydride catalyst to react with O_2. Introducing the mixture of $EtOH/H_2O/O_2$ into the reactor at 200 °C (or 230 °C, 0.03 g) resulted in an increase in temperature. The heating of the reactor was lowered as soon as the catalytic reaction started and the variation of temperature was measured.

Received: April 15, 2011
Revised: July 14, 2011
Published online: August 24, 2011

Keywords: ethanol · heterogeneous catalysis · hydrogen · metal oxides · sustainable chemistry

[1] a) V. A. Goltsov, T. N. Veziroglu, L. F. Goltsova, *Int. J. Hydrogen Energy* **2006**, *31*, 153 – 159; b) A. Midilli, M. Ay, I. Dincer, M. A. Rosen, *Renewable Sustainable Energy Rev.* **2005**, *9*, 273 – 287.

[2] a) A. Haryanto, S. Fernando, N. Murali, S. Adhikari, *Energy Fuels* **2005**, *19*, 2098 – 2106; b) M. Ni, D. Y. C. Leung, M. K. H. Leung, *Int. J. Hydrogen Energy* **2007**, *32*, 3238 – 3247.

[3] a) A. Kowal, M. Li, M. Shao, K. Sasaki, M. B. Vukmirovic, J. Zhang, N. S. Marinkovic, P. Liu, A. I. Frenkel, R. R. Adzic, *Nat. Mater.* **2009**, *8*, 325 – 330; b) F. Frusteri, S. Freni, V. Chiodo, S. Donato, G. Bonura, S. Cavallaro, *Int. J. Hydrogen Energy* **2006**, *31*, 15, 2193 – 2199; c) C. Resini, M. C. H. Delgado, S. Presto, L. J. Alemany, P. Riani, R. Marazza, G. Ramis, G. Busca, *Int. J. Hydrogen Energy* **2008**, *33*, 3728 – 3735; d) C. Lamy, S. Rousseau, E. M. Belgsir, C. Coutanceau, J.-M. Leger, *Electrochim. Acta* **2004**, *49*, 3901 – 3908; e) E. Antolini, *J. Power Sources* **2007**, *170*, 1 – 12.

[4] a) G. Zhou, L. Barrio, S. Agnoli, S. D. Senanayake, J. Evans, A. Kubacka, M. Estrella, J. C. Hanson, A. Martínez-Arias, M. Fernández-García, J. A. Rodriguez, *Angew. Chem.* **2010**, *122*, 9874 – 9878; *Angew. Chem. Int. Ed.* **2010**, *49*, 9680 – 9684; b) C. Resini, T. Montanari, L. Barattini, G. Ramis, G. Busca, S. Presto, P. Riani, R. Marazza, M. Sisani, F. Marmottini, U. Costantino, *Appl. Catal. A* **2009**, *355*, 83 – 93.

[5] a) J. R. Salge, G. A. Deluga, L. D. Schmidt, *J. Catal.* **2005**, *235*, 1, 69 – 78; b) S. N. Hsu, J. L. Bi, W. F. Wang, C. T. Yeh, C. B. Wang, *Int. J. Hydrogen Energy* **2008**, *33*, 2, 693 – 699.

[6] a) G. A. Deluga, J. R. Salge, L. D. Schmidt, X. E. Verykios, *Science* **2004**, *303*, 993 – 997; b) S. Velu, N. Satoh, C. S. Gopinath, K. Suzuki, *Catal. Lett.* **2002**, *82*, 1 – 2, 145 – 152; c) H. Chen, H. Yu, F. Peng, H. Wang, J. Yang, M. Pan, *J. Catal.* **2010**, *269*, 281 – 290; d) O. Akdim, W. Cai, V. Fierro, H. Provendier, A. van Veen, W. Shen, C. Mirodatos, *Top. Catal.* **2008**, *51*, 22 – 38; e) S. M. De Lima, I. O. da Cruz, G. Jacobs, B. H. Davis, L. V. Mattos, F. B. Noronha, *J. Catal.* **2008**, *257*, 356 – 368; f) J. Kugai, V. Subramani, C. Song, M. H. Engelhard, Y. H. Chin, *J. Catal.* **2006**, *238*, 430 – 440; g) W. J. Cai, F. G. Wang, E. S. Zhan, A. C. Van Veen, C. Mirodatos, W. J. Shen, *J. Catal.* **2008**, *257*, 96 – 107.

[7] a) L. Jalowiecki-Duhamel, C. Pirez, M. Capron, F. Dumeignil, E. Payen, *Int. J. Hydrogen Energy* **2010**, *35*, 12741 – 12750; b) L. Jalowiecki-Duhamel, C. Pirez, M. Capron, F. Dumeignil, E. Payen, *Catal. Today* **2010**, *157*, 456 – 461.

[8] a) C. Lamonier, A. Ponchel, A. D'Huysser, L. Jalowiecki-Duhamel, *Catal. Today* **1999**, *50*, 247 – 259; b) L. Jalowiecki-Duhamel, *Int. J. Hydrogen Energy* **2006**, *31*, 191 – 195; c) L. Jalowiecki-Duhamel, J. Carpentier, A. Ponchel, *Int. J. Hydrogen Energy* **2007**, *32*, 2439 – 2444; d) L Jalowiecki-Duhamel, H. Zarrou, A. D'Huysser, *Int. J. Hydrogen Energy* **2008**, *33*, 5527 – 5534.

[9] S. Kacimi, D. Duprez, J. A. Dalmon, *J. Chim. Phys. Biol.* **1997**, *94*, 535 – 552.

[10] H. Jobic, *Handbook of Heterogeneous Catalysis*, *2nd ed.* (Eds. G. Ertl, H. Knözinger, F. Schüth, J. Weitkamp), Wiley-VCH **2008**, 971.

[11] L. Jalowiecki-Duhamel, S. Debeusscher, H. Jobic, E. Payen, *Int. J. Nuclear Hydrogen Production and Applications* **2009**, *2*, 148 – 158.

[12] L. Barrio, A. Kubacka, G. Zhou, M. Estrella, A. Martinez-Arias, J. C. Hanson, M. Fernández-Garcia, J. A. Rodriguez, *J. Phys. Chem. C* **2010**, *114*, 12689 – 12697.

